Journal of Crystal Growth 507 (2019) 255–259

Contents lists available at ScienceDirect

Journal of Crystal Growth

journal homepage: www.elsevier.com/locate/jcrysgro

# Highly tin doped GaAs at low growth temperatures using tetraethyl tin by metal organic vapor phase epitaxy

Omar Elleuch*, Kaddour Lekhal, Yingxin Guan, Thomas F. Kuech

*University of Wisconsin, 1415 Engineering Drive, Madison, WI 53706-1691, USA*

ARTICLE INFO

Communicated by Yasuyuki Miyamoto

*Keywords:*
A3. Metalorganic vapor phase epitaxy
A1. Doping
A1. Segregation
B2. Semiconducting III-V materials

ABSTRACT

GaAs layers with a high tin (Sn) doping concentration and a smooth surface morphology were successfully grown at temperatures as low as 425 °C using tetraethyl tin (TESn) by metal organic vapor phase epitaxy (MOVPE). The samples grown at 650 °C showed Sn-rich droplets even with a low TESn molar flow rate of 0.06 µmol/min, indicating that Sn atoms were not incorporated into the GaAs film but segregated and accumulated on the film surface. Droplet formation was suppressed at a low growth temperature of 425 °C. This suggests that the segregation process is kinetically-limited, with the segregation mechanism is slow compared to the growth rate at low growth temperatures. Uncorrected Hall effect measurements found an electron concentration of $\sim 1 \times 10^{19}$ cm$^{-3}$, which is close to the maximum reported doping-limit obtainable in GaAs:Sn grown by MOVPE, while avoiding droplet formation and maintaining a smooth surface morphology. The electron mobility is dominated by the ionized impurity scattering. The sample possesses a generally flat Sn profile extending from the substrate to the film surface. Secondary ion mass spectroscopy indicates that the Sn is electrically active but compensated by carbon acceptors to yield the measured carrier concentration.

## 1. Introduction

Heavily-doped GaAs is a key technology in the fabrication of high-performance AlGaAs/GaAs heterojunctions bipolar transistors (HBTs) [1–8]. High doping concentrations offer low contact resistance in the emitter and the collector regions, low heat dissipation, and short RC time constants, thus increasing the speed of the device. The heavily-doped layers with a doping concentration on the order of $10^{19}$ cm$^{-3}$ or higher are desirable. The commonly used n-type dopants for GaAs are sulfur (S), selenium (Se), tellurium (Te), silicon (Si), and tin (Sn). However, the diffusion of S [9–13], and Se [14,15] exhibited a complex double-profile shape. Te doping suffers from the superdilation of the lattice at a carrier concentration above $2 \times 10^{18}$ cm$^{-3}$, where the lattice parameter increases with doping at a rate which is 15 times that given by Vegard's law prediction [16,17] indicative of the co-incorporation of point defects. In addition, Te has a very low sticking coefficient when using molecular beam epitaxy (MBE) due to the low condensation coefficients and/or low adsorption lifetimes, thus its incorporation has not been readily successful by MBE [18,19]. The highest available carrier concentration reported with Si is only $6 \times 10^{18}$ cm$^{-3}$ due to its amphoteric behavior and its limited solid solubility [20–22].

Sn is an alternative dopant that can overcome several of these disadvantages of the other dopants because: (i) it is less amphoteric than Si, (ii) can achieve a carrier concentration ~ 2x higher than Si, at > $10^{19}$ cm$^{-3}$, yielding one of the highest, if not the highest, n-type carrier concentrations in GaAs [23], and (iii) Sn has a lower vapor pressure than S, Se, and Te, which decreases the 'memory effect' [24]. Sn doping does have some complexities. Sn can exhibit concentration dependent diffusion, leading to the 'double knee' profile seen with Zn and other dopants at high carrier concentrations and high temperatures for extended times [25]. Sn can also exhibit surface segregation and subsequent accumulation due to solubility limitations under certain growth conditions. The reported carrier concentration for Sn doping when using metal organic vapor phase epitaxy (MOVPE) has, however, been much higher than other dopants with reported carrier concentrations of as high as $1.6–1.7 \times 10^{19}$ cm$^{-3}$ [26]. Typically, there is limited thermodynamic solubility for many dopants, such as Sn, which can lead to surface segregation. There was significant Sn segregation reported in this study for a growth temperature of 650 °C. A previous report showed that the surface segregation of Sn in GaAs can be significant at growth temperatures > 490 °C and with the degree of surface accumulation increasing with growth temperature [27]. Film growth at temperatures lower than 490 °C is an approach to suppress the surface segregation of Sn and to obtain highly doped layers possessing a low contact resistance without anomalous diffusion. Here,

* Corresponding author.
*E-mail address:* elleuch@wisc.edu (O. Elleuch).

https://doi.org/10.1016/j.jcrysgro.2018.11.021

Available online 22 November 2018

ethyl-based growth sources, triethyl gallium (TEGa) and tetraethyl tin (TESn), as an alternative to the more commonly employed trimethyl gallium (TMGa) and tetramethyl tin (TMSn), are employed to form high quality and heavily-doped GaAs films grown at low growth temperatures. TEGa has been used to deposit low carbon, high-purity GaAs epilayers at temperatures lower than typically achieved using TMGa [28,29]. Compared with TMSn, TESn has a lower decomposition temperature well-suited to low temperature growth and a suitable vapor pressure, which offer the possibility of growing n-type GaAs over a large range of dopant concentration.

In this paper, GaAs layers with high tin-doping concentration, smooth surface morphology, and controlled tin profile were successfully grown at low temperature of 425 °C using TEGa and TESn by MOVPE. The electron concentration obtained by uncorrected Hall-effect measurements is $\sim 1.0 \times 10^{19}$ cm$^{-3}$. The ionized impurity scattering dominates the electron mobility. The doping profiles of Sn is flat without observed segregation to the surface.

## 2. Experimental procedure

GaAs:Sn films were grown on nominally singular (1 0 0) GaAs substrates within a horizontal MOVPE reactor. The reactor pressure was 0.1 bar and the growth temperatures were 650 and 425 °C. Triethyl gallium ($(C_2H_5)_3Ga$), arsine ($AsH_3$), and tetraethyl tin ($(C_2H_5)_4Sn$) were used as the Ga, As, and Sn precursors, respectively. The molar flow rates for $(C_2H_5)_3Ga$ and $AsH_3$ are 60.6 and 822 µmol/min. The molar flow rates of $(C_2H_5)_4Sn$ are 0.06, 0.13, 0.25, 3.80, 7.60, 10.8 and 13.2 µmol/min. The sample structure is shown in the inset of Fig. 1. The growth of GaAs:Sn layer was preceded by the growth of a 1 µm-thick AlGaAs and a 100 nm-thick undoped GaAs buffer layer at 700 °C with an $AsH_3$ flow of 3288 µmol/min. The secondary ion mass spectroscopy data of preliminary samples showed Sn spike at the interface between GaAs:Sn layer and buffer layer. The use of AlGaAs layer eliminated the Sn spike at the interface and an uniform doping profile was obtained along the GaAs:Sn layer (see Fig. 3). The top GaAs buffer layer electrically isolates the AlGaAs layer and eliminates the possibility of the formation of a 2DEG at the GaAs-AlGaAs interface arising from the Sn doping. A hydrogen carrier gas was used at a total flow rate of ~ 7 slpm ( ~ 0.28 mol/min) within the 76 mm diameter horizontal reactor. Purified $H_2$ carrier gas was used. A growth time of 263 s was kept constant for all samples.

Carrier concentration and mobility were measured at room temperature using the Hall effect by the Van der Pauw method. The surface morphology and thickness of the samples was characterized by scanning electron microscopy (SEM) and atomic force microscope (AFM). Secondary ion mass spectroscopy (SIMS) was used to obtain the atomic concentrations of Sn and C in GaAs epilayers allowing a general comparison of the physical and electrically-active Sn concentrations. SIMS measurement was performed using 14.5 keV $Cs^+$ primary ions.

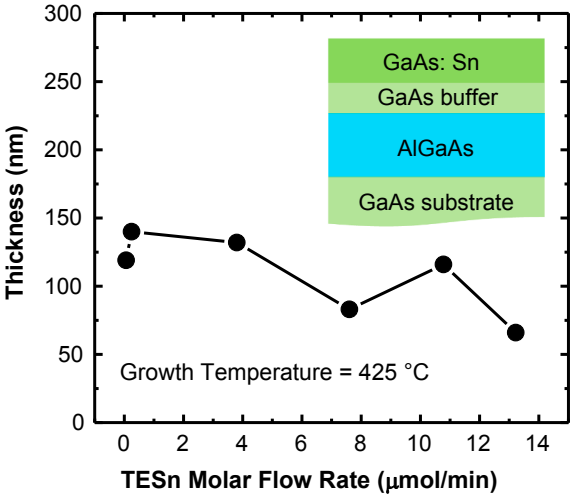


**Fig. 1.** The GaAs:Sn film thickness (growth rate) dependence on the TESn molar flow rate. The growth time and growth temperature were fixed at 263 sec and 425 °C, respectively.

## 3. Experimental results

The TESn molar flow rate dependence of the thicknesses of GaAs:Sn films grown at 425 °C is illustrated in Fig. 1. The thickness decreases when the TESn molar flow rate increases. The decrease in the growth rate at high TESn flow rate indicates an influence of the Sn or some component of the TESn in modifying the growth front chemistry.

The surface morphology of Sn-doped GaAs films grown at 650 and 425 °C is shown in Fig. 2. At 650 °C, Sn droplets exist with a low TESn molar flow rate of 0.13 µmol/min evidencing surface segregation with subsequent surface accumulation and aggregation. Rough or non-planar surface morphology has been reported, even without Sn droplet formation in several previous MOVPE studies, particularly at high doping levels [30], for layers grown ~625–685 °C. Both SEM and AFM images reveal that the growth at lower temperature led to a smooth morphology with no Sn droplet formation even at the highest achieved doping level, where the RMS roughness is < 1 nm with values of 0.32 and 0.52 nm at TESn = 0.13 and 13.22 µmol/min, respectively.

The concentrations of Sn and C in GaAs:Sn grown at 425 °C are shown in Fig. 3. The sample shows a generally flat Sn profile extending from the substrate to the film surface. The Sn and C concentrations are around $2.1 \times 10^{19}$ and $1 \times 10^{19}$ cm$^{-3}$, respectively. The C concentration in the GaAs:Sn film is higher than in GaAs buffer layer. A primary reason is the difference in growth temperatures, which are 425 and 700 °C for GaAs:Sn and GaAs buffer, respectively. The decomposition of organometallic sources in MOVPE is thermally activated and when the temperature is low the decomposition efficiency decreases, leading to a higher C concentration. In addition, the decomposition of TESn may also lead to extraneous C in the GaAs:Sn film.

The carrier concentration as a function of TESn molar flow rate for GaAs:Sn films grown at 425 °C is shown in Fig. 4. If the carrier concentration was defined as $n = \frac{-1}{eR_H}$, where $R_H$ is the measured Hall coefficient, there will be an underestimate of both the carrier concentration and the mobility. In the case of mobility, there is generally a ~30% underestimate of the mobility using the conventional, uncorrected Hall measurements. In the case of degenerate semiconductors, the carrier transport is dominated by ionized impurity scattering, as is the case here, and the band structure is modified by impurity banding and other band structure modifications. The Hall coefficient is more accurately defined as $R_H = \frac{-1}{ne}\frac{\langle\tau^2\rangle}{\langle\tau\rangle^2}$ where $\frac{\langle\tau^2\rangle}{\langle\tau\rangle^2}$ is the appropriate averages of the energy dependent carrier scattering factor, $\tau(\varepsilon)$ [31]. The typical case where lattice scattering dominates $\left(\tau(\varepsilon) \propto \varepsilon^{-\frac{1}{2}}\right)$ in non-degenerate, high temperature measurements, $\frac{\langle\tau^2\rangle}{\langle\tau\rangle^2} = \frac{3\pi}{8}$ which is generally set equal to unity. For cases where impurity scattering dominates $\left(\tau(\varepsilon) \propto \varepsilon^{\frac{3}{2}}\right)$, as in the current measurements, $\frac{\langle\tau^2\rangle}{\langle\tau\rangle^2} = \frac{315\pi}{512} = 1.93$. The real case is yet more complicated by the presence of impurity bands and potentially non-parabolic bands. This indicates that the actual carrier concentration is substantially higher than indicated by the simplest interpretation of the Hall measurements. Similar modifications and concerns over the interpretation of the mobility derived from the Hall measurement must be taken [32,33]. In this paper we will use the corrected Hall coefficient, i.e. $R_H = \frac{-1.93}{en_e}$, to provide a more accurate estimate of the carrier concentration relevant for device applications.

All films were highly *n*-type as grown. The electron concentration, $n_e$, increases with TESn molar flow rate then saturates due to both

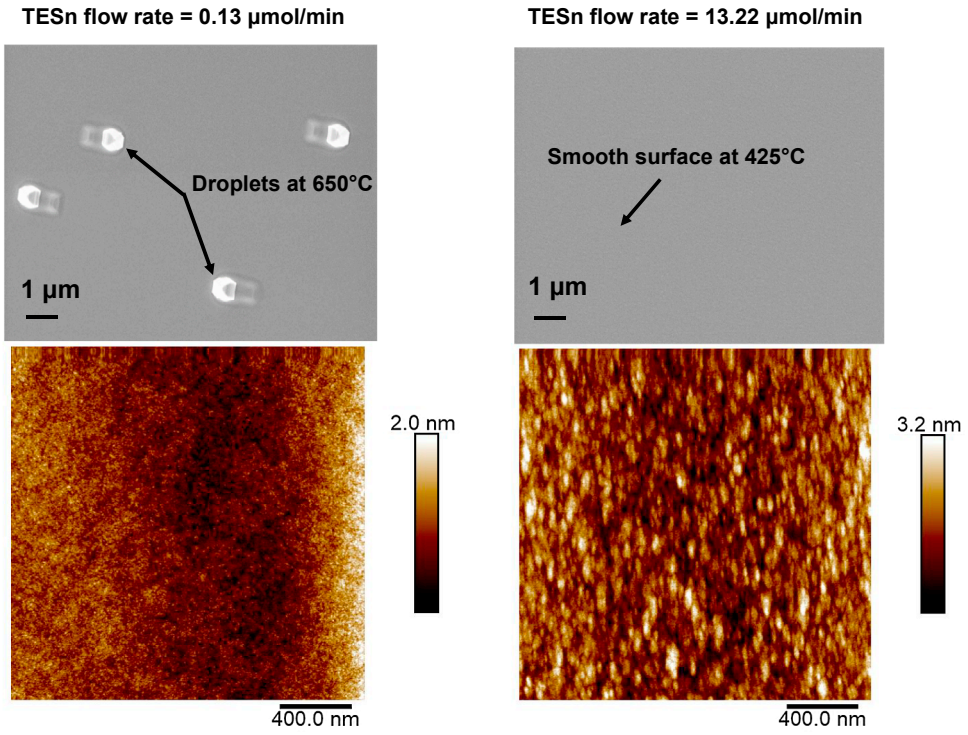


**Fig. 2.** Surface morphology of GaAs:Sn films grown at 650 and 425 °C. The TESn molar flow rates are 0.13 and 13.22 µmol/min, respectively. Sn droplets appear at 650 °C but are suppressed at a growth temperature of 425 °C. The RMS roughness for both samples is < 1 nm with values of 0.32 and 0.52 nm at TESn = 0.13 and 13.22 µmol/min, respectively.

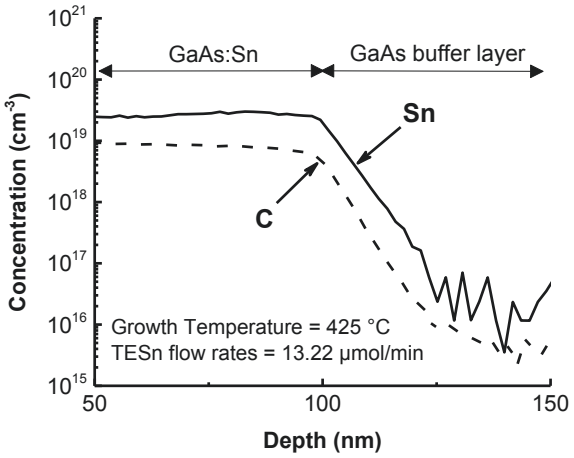


**Fig. 3.** SIMS-based measurement of the Sn and C concentrations in a typical GaAs:Sn layer grown at 425 °C.

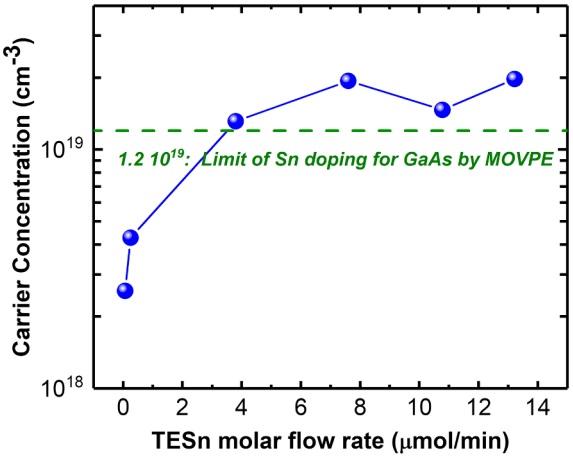


**Fig. 4.** Carrier concentration versus the TESn molar flow rate for GaAs:Sn films grown at 425 °C assuming a Hall coefficient corrected as outlined in text.

approaching the dopant solubility and perhaps limitations due to surface incorporation at these high TESn flow rates and low growth temperatures. At some point, the Fermi level is pulled sufficiently far from the impurity band that further ionization is not possible with increased dopant incorporation. A value of $n_e = 2.00 \times 10^{19}$ cm$^{-3}$ was achieved, which is among the highest reported for MOVPE growth without surface segregation [24,26] and higher than the reported solid solubility at this temperature, also indicated on the graph. The smooth surface morphology was preserved even at the high doping level. In this work, the use of TESn offers not only a high electron concentration, but also allow the low temperature growth, which is beneficial in the growth of other materials systems which cannot support the high temperature growth.

Fig. 5 shows the electron mobility, $\mu_e$, versus the carrier concentration at room temperature. $\mu_e$ decreases with increases in Sn, and hence, electron concentration. The mobility would be dominated by ionized impurity scattering at these doping levels. A mobility of 978 cm$^2$.V$^{-1}$s$^{-1}$ is achieved at the highest doping concentration of $\sim 2 \times 10^{-19}$ cm$^{-3}$. This is similar to ones reported in GaAs:Sn films grown by MOVPE [24,34]. The low-temperature growth of Sn-doped GaAs present drawbacks such as the incorporation of high density of carbon. However, the mobility is high enough to be acceptable for device fabrication [1]. Further works will be carried out to study the effect of defects and impurities on device performance.

## 4. Discussion

The solubility of Sn in GaAs has been discussed in the literature, particularly for melt-grown GaAs:Sn and liquid phase epitaxy (LPE) materials grown from a Ga-rich melt [35,36]. The Sn segregation coefficient, $k_{Sn}$, i.e. the ratio of Sn in the solid to Sn in the liquid, in LPE was a function of temperature and typical quite low on the order of $k_{Sn} \approx 10^{-4}$ at 700–800 °C [37–39]. Similar values are predicted, $k_{Sn} = 4 \times 10^{-3}$ [40], and seen for bulk grown GaAs however at much higher temperatures.

There have been estimates of the vapor phase segregation

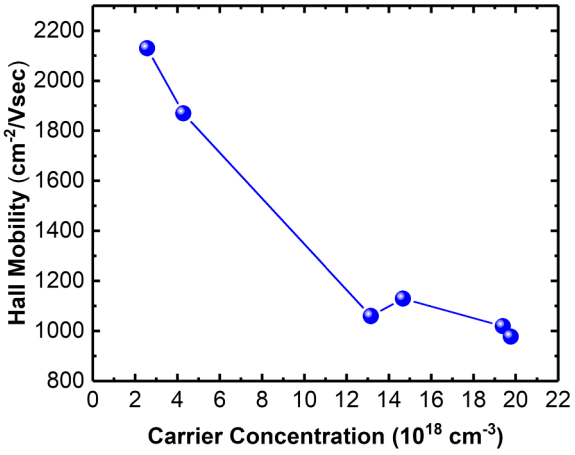


**Fig. 5.** Room temperature electron mobility, $\mu_e$, as a function of carrier concentration.

coefficient as well for both molecular beam epitaxy (MBE) and MOVPE. Thermodynamics estimates for MBE and MOVPE indicate that the measured Sn concentrations are far in excess of those predicted and hence kinetic processes are seen to dominate the Sn-incorporation process at low growth temperatures [41–43]. The low segregation coefficients indicate that the Sn incorporation process occurs from an absorbed layer or layers of Sn on the surface. Sn is initially rejected from the film until a steady-state surface layer is developed. This has been demonstrated in surface science and MBE growth studies [44,45] and is expected to be present in MOVPE.

The results of the present study, as well as the previously cited MBE studies, indicate that low growth temperatures allow for the incorporation of Sn well-above the thermodynamic solubility limit. In all cases, it is anticipated that there exists a monolayer or more of Sn on the surface which serves as a reservoir of Sn during growth. The kinetic models developed for the case of MBE rely on impurity trapping at the growth front by the growing film leading to Sn incorporation of Sn and preventing macroscopic accumulation on the surface. We expect similar mechanisms at these temperatures for MOVPE.

The thermodynamic analysis of the point defect structure of Sn-doped GaAs has been carried out by Hurle [46,47]. The partial compensation of the Sn, as a simple donor, $Sn_{Ga}^{+}$, has been attributed to the thermodynamically favored formation of an acceptor defect complex, $Sn_{Ga}V_{Ga}^{-}$, as well as unintentional carbon acceptors. The choice of specific compensating point defects also depends on the specific As activity at the growth front which is difficult to ascertain within the MOVPE system. The SIMS data also indicates the presence of carbon which are assumed to be acceptors.

## 5. Conclusions

A controlled electron concentration with a smooth morphology and controlled doping profile were successfully grown at low temperature (425 °C) using TESn by MOVPE, where a carrier concentration of $> 10^{19}$ cm$^{-3}$ has been achieved. This establishes TESn doping as an efficient doping platform for GaAs at low growth temperature potentially extendable to other materials systems requiring a low growth temperature.

## Acknowledgments

This research was primarily supported by NSF Division of Materials Research through the University of Wisconsin Materials Research Science and Engineering Center (DMR-1720415).

## References

[1] H. Ito, T. Ishibashi, Heavily Sn-doped GaAs buffer layers for AlGaAs/GaAs HBTs, Jpn. J. Appl. Phys. 27 (1988) L707–L709.
[2] K.C. Wang, P.M. Asbeck, M.F. Chang, G.J. Sullivan, D.L. Miller, A 20-GHz frequency divider implemented with heterojunction bipolar transistors, IEEE Electron Device Lett. 8 (1987) 383–385.
[3] Y. Yamauchi, K. Nagata, O. Nakajima, H. Ito, T. Nittono, T. Ishibashi, 22 GHz 1/4 frequency divider using AlGaAs/GaAs HBTs, Electron. Lett. 23 (1987) 881–882.
[4] M.F. Chang, P.M. Asbeck, K.C. Wang, G.J. Sullivan, N.H. Sheng, J.A. Higgins, D.L. Miller, AlGaAs/GaAs heterojunction bipolar transistors fabricated using a self-aligned dual-lift-off process, EDL-8, IEEE Electron Device Lett. (1987) 303–305.
[5] K. Nagata, O. Nakajima, Y. Yamauchi, H. Ito, T. Nittono and T. Ishibashi, High-Speed Performance of Al1-xGaxAs/GaAs Heterojunction Bipolar Transistors with Nonalloyed Emitter Contacts, in Proceedings of the 45th Annual Device Research Conf., Santa Barbara, CA, June 22-24, 1987, pp. IVA-2.
[6] T. Ishibashi, Y. Yamauchi, O. Nakajima, K. Nagata, H. Ito, High-speed frequency dividers using self-aligned AlGaAs/GaAs heterojunction bipolar transistors, IEEE Electron Device Lett. (1987) 194–196.
[7] P.M. Asbeck, D.L. Miller, R.J. Anderson, R.N. Deming, R.T. Chen, C.A. Liechti, F.H. Eisen, Application of heterojunction bipolar transistor to high speed, small-scale digital integrated circuits, in Proc. GaAs I.C. Symp., Oct. 1984, pp. 133-136.
[8] K.C. Wang, P.M. Asbeck, M.F. Chang, D.L. Miller, and G.J. Sullivan, High-speed MSI current-mode logic circuits implemented with heterojunction bipolar transistors, in Proc. GaAs I.C. Symp., 1986, pp. 159-162.
[9] M.D. Zahari, B. Tuck, Substitutional-interstitial diffusion in semiconductor, J. Phys. D: Appl. Phys. 18 (1985) 1585–1595.
[10] M.D. Zahari, B. Tuck, Effect of vacancy reduction on diffusion in semiconductors, J. Phys. D: Appl. Phys. 15 (1982) 1741–1750.
[11] O. Madelung, Semiconductors—Basic Data, second ed., Springer-Verlag, Berlin, 1996.
[12] M.D. Zahari, B. Tuck, Substitutional-interstitial diffusion with bulk vacancy generation in semiconductor, J. Phys. D: Appl. Phys. 16 (1983) 635–644.
[13] S.J. Bass, Device quality epitaxial gallium arsenide grown by the metal alkyl-hydride technique, J. Cryst. Growth 31 (1975) 172–178.
[14] R.W. Fane, A.J. Goss, The diffusion of tin and selenium in gallium arsenide, Solid-State Electron. 6 (1963) 383–387.
[15] H.M. Manasevit, W.I. Simpson, The use of metal-organics in the preparation of semiconductor materials, J. Electrochem. Soc. 116 (1969) 1725–1732.
[16] G.M. Kuznetsov, O.V. Pelevin, A.D. Barsukov, V.V. Olenin, I.A. Savel'eva, Sov. Phys. Crystallogr. 17 (1972) 539.
[17] J.B. Mullin, B.W. Straughan, C.M.H. Driscoll, A.F.W. Willoughby, Lattice superdilation phenomena in doped GaAs, J. Appl. Phys. 47 (1976) 2584–2587.
[18] C.D. Stinespring, A. Freedman, Surface chemistry of dimethyl cadmium and dimethyl tellurium at 295 K, Chem. Phys. Lett. 143 (1988) 584–588.
[19] W.S. Liu, Gregory B. Raupp, The Surface chemistry of CdTe Mocvd, Mat. Res. Soc. Symp. Proc. 334 (1994) 239–244.
[20] M. Ogawa, T. Baba, Heavily Si-doped GaAs and AlAs/n-GaAs superlattice grown by molecular beam epitaxy, Jpn. J. Appl. Phys. 24 (1985) L572–L574.
[21] C.R. Abernathy, S.J. Pearton, N.T. Ha, Sn doping of GaAs and AlGaAs grown by metalorganic molecular-beam epitaxy, J. Cryst. Growth 108 (1991) 827–830.
[22] N. Furuhata, K. Kakimoto, M. Yoshida, T. Kamejima, Heavily Si-doped GaAs grown by metalorganic chemical vapor deposition, J. Appl. Phys. 64 (1988) 4692–4695.
[23] C.R. Abernathy, S.J. Pearton, F. Ren, J. Song, Sn doping of GaAs and AlGaAs by MOMBE using tetraethyltin, J. Cryst. Growth 113 (1991) 412–416.
[24] J.D. Parsons, F.G. Krajenbrink, Tin doping of gallium arsenide by metal organic chemical vapor deposition (MOCVD), J. Electrochem. Soc. 130 (1983) 1780–1781.
[25] M.G. Debs, T.F. Kuech, Phenomenological modeling of diffusion profiles: Sn in GaAs, J. Appl. Phys. 99 (2006) 123710–1–123710-7.
[26] V.S. Sundaram, A.P. Roth, D.F. Williams, R. Yakimova, Surface accumulation of tin in tin-doped gallium arsenide grown by low pressure metalorganic vapor phase epitaxy, Appl. Phys. Lett. 45 (1984) 1196–1198.
[27] K. Ploog, A. Fischer, Surface segregation of Sn during MBE of n-type GaAs established by SIMS and AES, J. Vac. Sci. Technol. 15 (1978) 255–259.
[28] C. Plass, H. Heinecke, O. Kayser, H. Lüth, P. Balk, A comparative study of $Ga(CH_3)_3$, $Ga(C_2H_5)_3$ and $Ga(C_4H_9)_3$ in the low pressure MOCVD of GaAs, J. Crystal Growth 88 (1988) 455–464.
[29] Y. Seki, K. Tanno, K. Iida, E. Ichiki, Properties of epitaxial GaAs layers from a triethyl gallium and arsine system, J. Electrochem. Soc. 122 (1975) 1108–1112.
[30] R. Yakimova, A.P. Roth, D.F. Williams, V.S. Sundaram, Morphology of tin doped gallium arsenide grown by low pressure MOVPE, J. Cryst. Growth 68 (1984) 71–77.
[31] F. Blatt, Physics of Electronic Conduction in Solids, (McGraw-Hill, 1968, New York) Chap. 8.
[32] D.B. Agarwal, Hall mobility of degenerate semiconductors, Zeitschrift für Physik 163 (1961) 207–210.
[33] C.K. Williams, M.A. Littlejohn, T.H. Glisson, J.R. Hauser, Monte Carlo simulation of the hall effect in degenerate GaAs, Superlatt. Microstruct. 2 (1986) 201–207.
[34] J.D. Parsons, F.G. Krajenbrink, Tin doping of MOVPE grown gallium arsenide using tetraethyltin, J. Cryst. Growth 68 (1984) 60–64.
[35] M.R. Brozel, E.J. Foulkes, I.R. Grant, D.T.J. Hurle, Tin segregation and donor compensation in melt-grown gallium arsenide, J. Cryst. Growth 80 (1972) 323–332.
[36] D.T.J. Hurle, A comprehensive thermodynamic analysis of native point defect and dopant solubilities in gallium arsenide, J. Appl. Phys. 85 (1999) 6957–7022.
[37] E. Kuphal, A. Schlachetzki, A. Pöcker, Incorporation of Sn into epitaxial GaAs grown from the liquid phase, Appl. Phys. 17 (1978) 63–72.

[38] J. Vilms, J.P. Garrett, The growth and properties of LPE GaAs, Solid-State Electron. 15 (1972) 443–455.
[39] M.B. Panish, The system Ga–As–Sn: incorporation of Sn into GaAs, J. Appl. Phys. 44 (1973) 2659–2666.
[40] M.R. Brozel, E.J. Foulkes, I.R. Grant, D.T.J. Hurle, Tin segregation and donor compensation in melt-grown gallium arsenide, J. Cryst. Growth 80 (1987) 323–332.
[41] R. Heckingbottom, G.J. Davies, K.A. Prior, Growth and doping of gallium arsenide using molecular beam epitaxy (MBE): Thermodynamic and kinetic aspects, Surface Science 132 (1983) 375–389.
[42] S.V. Ivaniov, P.S. Kop'ev, N.N. Ledentsov, Thermodynamic analysis of segregation effects in molecular beam epitaxy, J. Crystal Growth 104 (1990) 345–354.
[43] L.C. Keizer, X. Tang, R.Z.C. Van Meerten, L.J. Giling, Doping of gallium arsenide in MOCVD: Equilibrium calculations, J. Crystal Growth 102 (1990) 667–677.
[44] C.E.C. Wood, B.A. Joyce, Tin-doping effects in GaAs films grown by molecular beam epitaxy, J. Appl. Phys. 49 (1978) 4854–4861.
[45] J.J. Harris, D.E. Ashenford, C.T. Foxon, P.J. Dobson, B.A. Joyce, Kinetic limitations to surface segregation during MBE growth of III–V compounds: Sn in GaAs, Appl. Phys. A 33 (1984) 87–92.
[46] D.T.J. Hurle, Solubility and point defect-dopant interactions in GaAs—II: Tin-doping, J. Phys. Chem. Solids 40 (1979) 639–646.
[47] D.T.J. Hurle, A thermodynamic analysis of native point defect and dopant solubilities in zinc-blende III–V semiconductors, J. Appl. Phys. 107 (2010) 121301–1–121301-47.